Ice Nucleation Activity of Iron Oxides via Immersion Freezing and an Examination of the High Ice Nucleation Activity of FeO

Esther Chong¹, Katherine E. Marak¹, Yang Li^{1,&}, and Miriam Arak Freedman^{1,*}

1) Department of Chemistry, The Pennsylvania State University, University Park, PA 16802

Accepted to Physical Chemistry Chemical Physics

*To whom all correspondence should be addressed: maf43@psu.edu, +01-814-867-4267

& Present address: Aquatic Ecology and Water Quality Management Group, Wageningen

University & Research, 6700 AA Wageningen, The Netherlands

ABSTRACT

Heterogeneous ice nucleation is a common process in the atmosphere, but relatively little is known about the role of different surface characteristics on the promotion of ice nucleation. We have used a series of iron oxides as a model system to study the role of lattice mismatch and defects induced by milling on ice nucleation activity. The iron oxides include wüstite (FeO), hematite (Fe₂O₃), magnetite (Fe₃O₄), and goethite (FeOOH). The iron oxides were characterized by X-ray diffraction (XRD) and Brunauer-Emmett-Teller (BET) surface area measurements. The immersion freezing experiments were performed using an environmental chamber. Wüstite (FeO) had the highest ice nucleation activity, which we attribute to its low lattice mismatch with hexagonal ice and the exposure of Fe-OH after milling. A comparison study of MnO and wüstite (FeO) with milled and sieved samples for each suggests that physical defects alone result in only a slight increase in ice nucleation activity. Despite differences in the molecular formula and surface groups,

hematite (Fe₂O₃), magnetite (Fe₃O₄), and goethite (FeOOH) had similar ice nucleation activities, which may be attributed to their high lattice mismatch to hexagonal ice. This study provides further insight into the characteristics of a good heterogeneous ice nucleus and, more generally, helps to elucidate the interactions between aerosol particles and ice particles in clouds.

INTRODUCTION

Ice nucleation impacts the microphysical and optical properties of clouds and, thus, the Earth's radiative budget. Without a solid particle, water droplets must be supercooled to -38 °C to undergo homogeneous ice nucleation. Heterogeneous nucleation allows ice to form at warmer temperatures in comparison.¹ A variety of aerosol particles such as mineral dust ^{2–6}, biogenic material ^{7–10}, and soot ^{11–13} are commonly found in the atmosphere and can act as ice nucleating particles. The ice nucleation activity of aerosol particles is widely variable, ¹⁴ however, due to the complexity of atmospheric aerosol particles and the sensitivity of ice nucleation activity to the surface properties of particles.

Among the general categories for ice nucleating particle, bacteria and other biogenic material have been found to have some of the highest ice nucleation activities. Mineral dust nucleates ice over a range of temperatures, with some of the most active beginning nucleation around -10 °C, which is significantly colder compared to biological nuclei that have been shown to nucleate ice as warm as -2 °C.^{7,15} Studies have shown that ice nucleating molecules, commonly proteins, are the main indicators for the ice nucleation activity of biological material.^{16–18} While aerosol particles have large spatial and temporal variations over the globe, the overall concentration of mineral dust has been observed to be much higher than biological material.¹⁹ The scarcity of biological material could be, in part, a result of ineffective *in situ* collection methods or the quick sedimentation of biological material because of their size and hygroscopicity.^{20,21}

In comparison to biological material, small mineral dust particles < 1.8 µm have been observed to have long atmospheric lifetimes.^{22,23} Lattice match and morphological defects are two properties of mineral dust aerosol that have been shown to impact ice nucleation activity.²⁴ The effect of lattice match between a heterogeneous nucleus and ice on ice nucleation has been extensively studied, primarily through modeling studies, though lattice spacing is often tied to other factors which influence ice nucleation activity, such as composition.^{25–30} Similar lattice spacings suggest that the crystal lattice of the particle can act as a template for water molecules to arrange that will facilitate the formation of an ice lattice and initiate ice nucleation. Studies have shown that good lattice match can be a contributing factor in ice nucleation activity but is not necessary. 25,26 Historically, AgI has been viewed as an example compound for ice nucleation with high lattice match with hexagonal ice, but additional research has found that surface charge can negate the ice nucleation activity. ^{31–34} In molecular dynamic (MD) simulations, a lattice mismatch boundary of 5.7% is defined, in which lower mismatch shows the highest ice nucleation activity, and a higher mismatch results in a sharp decrease in ice nucleation activity.³⁵ In addition, a high lattice match does not correlate directly to having good ice nucleation activity as shown with BaF₂, which has a high lattice match but nucleates ice at -15 °C, likely as a result of wettability and electrostatic charges at the BaF₂ surface.³⁶

Morphological defects on the surface can include physical defects such as pores, step-edges, and irregular shapes.^{3,37–41} A direct observation study has shown that ice nucleates along the cracks and other physical defects found on feldspars.⁴² Along these defects, the studies suggest that confined water in the wedges/cracks as well as the arrangement of hydroxyl groups in these defects may promote ice nucleation.^{3,43} In addition, surface features have been shown to arise from the phase separation of Na⁺ and K⁺-rich domains. The resulting topographical surface features were

proposed to be important ice nucleation sites of alkali feldspars.⁴⁴ Defects can be native to the structure of the material, but they can also be introduced with mechanical processing. For ice nucleation experiments, the studied material is often processed, which can create defects. The defects may expose functional groups that would not be otherwise available. Hiranuma et al. observed an order of magnitude increase in the ice nucleation activity for milled hematite compared to the unprocessed hematite.⁴⁵ Similarly, Zolles et al. found that milled quartz followed a similar trend.⁴⁶ In both studies, it was speculated that the milling created physical defects with a possible change in the surface site density of functional groups.^{45,46}

Atmospheric particles are complex systems that have undergone both chemical and physical processing. As such, determining which properties of a particle affect its ice nucleation activity can be difficult to narrow down. Alternately, simple model systems can be studied to control as many variables as possible and investigate the effect of specific surface properties. In a previous study, we have examined the effect of crystallinity and crystal structure on the ice nucleation of alumina samples.⁴⁷ In this paper, we have characterized iron oxides as a model system with similar compositions and high crystallinity to explore the effect of crystal structure and surface functional groups on ice nucleation activity. Of the iron oxides studied, hematite (Fe₂O₃) and goethite (FeOOH) are the most commonly found in nature with hematite found in rock deposits and goethite in soils.⁴⁸ Magnetite (Fe₃O₄) is found as a component in igneous rocks.⁴⁹ Although wüstite (FeO) is rarely found naturally above the Earth's lower mantle because of its instability at temperatures below 570 °C, an ambient temperature-stable, synthetic wüstite (FeO) sample is purchasable from manufacturers and thus, was added to the study as an additional iron oxide to compare. 50,51 With the exception of wüstite, iron oxides are often found as components in mineral dust aerosol, especially Saharan dust.⁵² In addition, iron-containing mineral dust has been

widely studied because it has been hypothesized to be an important source of iron for ocean biogeochemistry.^{53–56} As a common compound in mineral dust, iron oxide can undergo reactions in the ocean as well as in the atmosphere. Processing in the atmosphere has been shown to improve the solubility of iron aerosol particles which are then available for absorption by primary producers in the ocean.^{57,58} This study focuses on the ice nucleation of iron oxide as a model system to understand the ice nucleation of compositionally complex mineral dust. Thus, the iron oxide system allows us to study the effect of lattice match, physical defects, and functional groups at the surface on ice nucleation activity.

EXPERIMENTAL METHODS

The iron oxide samples were purchased from Sigma Aldrich (FeO ≥99.6% (large crystals), Fe₂O₃ ≥99.9% (spherical), Fe₃O₄ 97% (spherical), FeOOH 30-63% Fe (leaf-like crystal aggregates)), and MnO (large crystals) was purchased from Acros Organics (99.99%). X-ray diffraction (XRD) was used to determine the purity and crystallinity of the iron oxide samples. The diffractograms were taken on a Malvern Panalytical Empyrean with Co Kα radiation with a current of 40 mA and a voltage of 40 kV. The powder samples were loaded onto a background silicon holder. The goniometer angles were set from 5.54 to 84° 2θ with a scan step time of 24.765 s. The XRD diffractograms were analyzed using Jade XRD libraries and whole pattern fitting. BET analysis with nitrogen gas was performed on an ASAP 2020 Automated Surface Area and Porosimetry System to determine the surface area of each sample.⁵⁹ The hydroxyl and oxygenmetal surface groups on the iron oxides were determined with X-ray photoelectron spectroscopy (XPS) using a Physical Electronics VersaProbe II. The instrument was equipped with a monochromatic Al Kα X-ray source and a concentric hemispherical analyzer. Low energy

electrons and argon ions were used for charge neutralization. Calibration of the binding energy axis was performed using sputter cleaned Cu and Au foils.

Immersion freezing data were taken using an environmental chamber described in detail in Alstadt et al. 60 Briefly, 2 µL droplets of 0.02 wt. % of iron oxide powder in UHPLC-MS water (Fisher Scientific) were pipetted onto silanized slides (Hampton Research). The iron oxide powders were generally used as they came from the manufacturer; however, FeO required milling for the powder to be small enough to be dispersed in solution. Milling the other iron oxide samples would not further reduce their sizes, nor would we expect changes in their physical or chemical properties. The milling was done on a McCrone Micronizing Mill. The sieved FeO and MnO samples were passed through a 20 µm sieve. The sieved and milled FeO look similar when imaged with scanning electron microscopy. Both surfaces are smooth with few defects, although the milled sample has scattered jagged edges. Unless stated otherwise, all wüstite (FeO) data was performed with milled wüstite (FeO) that was less than one week old. Results from XRD show that the mineral is stable in structure over this time period. Then, the slides were placed into the ice nucleation chamber. Pictures were taken every 0.5 °C as the chamber was cooled by liquid N₂ at a cooling rate of 3 °C/min. The chamber has a continuous steady stream of purified N₂ gas to prevent condensation and ice formation on the cooling block.

For each 0.5 °C interval, the frozen droplets were visually counted to calculate the frozen fraction with a minimum sample size of 240 droplets. The cumulative frozen fraction (f_{ice}) was calculated according to the equation

$$f_{\text{ice}} = \frac{n(T)}{N} \tag{1}$$

where n(T) is the total number of frozen droplets at a given temperature, and N is the total number of droplets in the sample population. Background water (homogeneous) freezing and surface area

differences between the iron oxide samples were used to normalize the frozen fraction data. K(T), the number of nucleation sites per milliliter of water at a specific temperature for each trial, was then calculated. The equation for K(T) is given by:

$$K(T) = \frac{-\ln\left[1 - F(T)\right]}{V} \times d \tag{2}$$

where F(T) is the fraction of droplets frozen at a specific temperature, V is the drop volume in milliliters, and d is the dilution factor. The K(T) for Millipore water was subtracted from the K(T) of each iron oxide data set. Then, the cumulative number of surface sites per unit area as a function of temperature (n_s) was calculated from K(T) using the equation

$$n_{s} = K(T) \times C^{-1} \tag{3}$$

where C is the total surface area of iron oxide in a given volume. C was calculated from the BET surface area and the weight percent of the iron oxide samples prepared for immersion freezing. For each average K(T), the n_s was calculated with the standard deviation calculated using the standard deviation of the calculated K(T) of each trial. Error in n_s is represented by the standard deviation between the trials, typically 8 trials at minimum were used for each sample.

Lattice mismatch between the iron oxide samples and hexagonal ice was calculated. The following equation was used to calculate the lattice mismatch (δ) along an axis:

$$\delta = \frac{a_{0,S} - a_{0,i}}{a_{0,i}} * 100 \tag{4}$$

where $a_{\theta, S}$ is the lattice constant of the substrate, and $a_{\theta, i}$ is the bulk lattice constant of ice I_h. A high value of δ indicates a poor lattice match and a higher level of strain on the bulk ice templating on the substrate.

RESULTS & DISCUSSION

From the XRD diffractograms found in Figure 1, all the iron oxide samples were found to be highly crystalline. The high crystallinity is evident from the narrow peaks and low background

noise. Other studies have found that crystallinity can affect ice nucleation activity.^{47,62} Bi et al. used molecular dynamic simulations and observed that a combination of the crystallinity of the graphitic surface and the strength of the water-carbon interaction directly influenced the ice nucleation activity. A crystalline surface with a sufficient water-carbon interaction strength will induce templating for the water molecules and create a strained ice lattice.⁶² In addition, the surface area of the iron oxides was measured using BET (Table 1). The porosity of these samples is negligible as determined from the BET characterization.

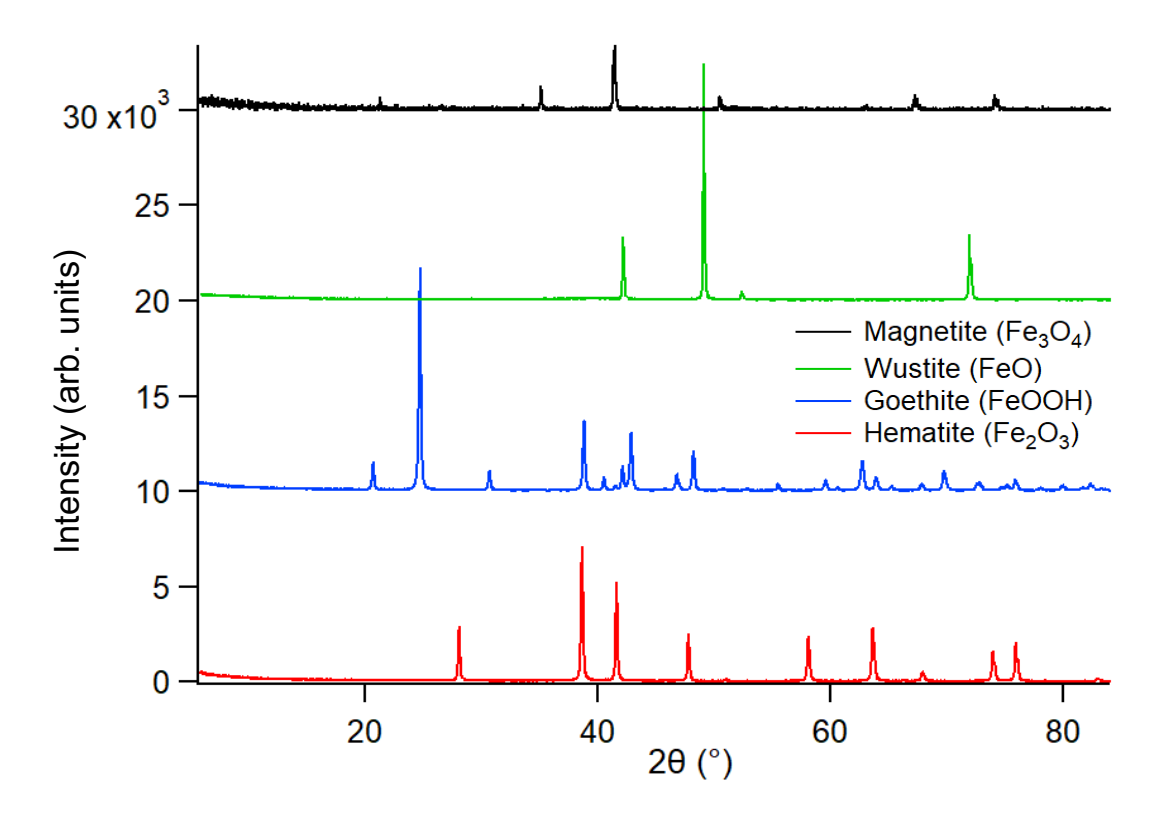


Figure 1. The diffractograms of the iron oxide samples. The wüstite (FeO) sample was milled. The diffractograms of the different samples are offset for clarity.

Table 1. The BET analysis of the iron oxide samples shown with uncertainty from the instrument.

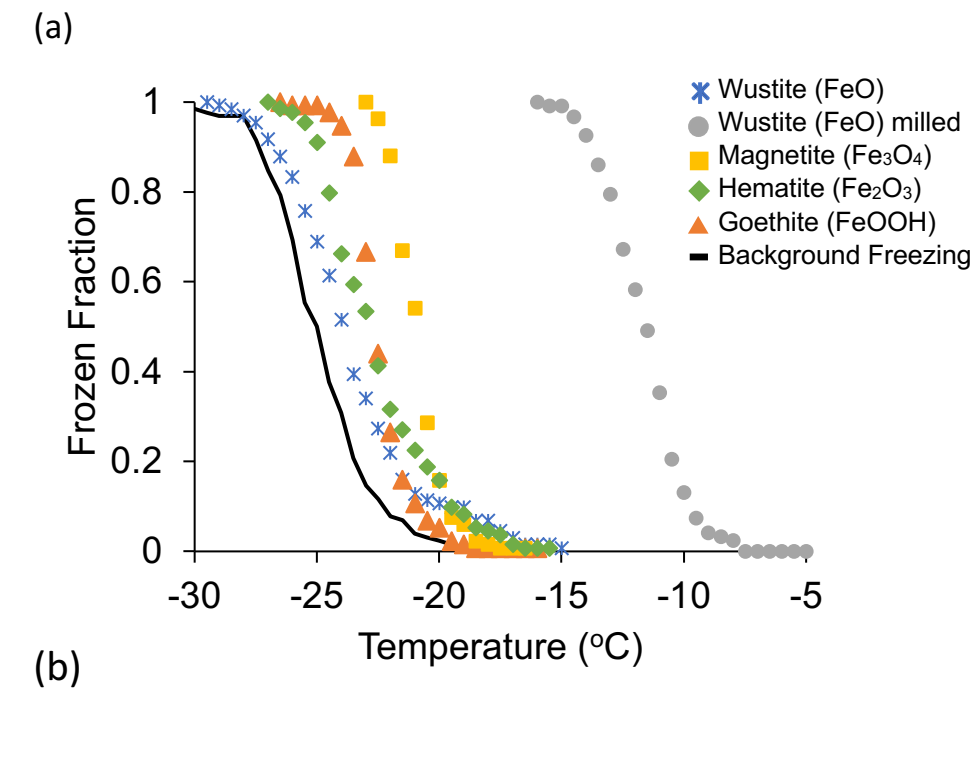
Sample	Surface Area (m ² /g)
Wüstite	
[FeO]	0.86 ± 0.02
(mill)	

Wüstite [FeO] (20 µm sieve)	0.55 ± 0.05
Hematite [Fe ₂ O ₃]	5.86 ± 0.02
Magnetite [Fe ₃ O ₄]	7.79 ± 0.03
Goethite [FeOOH]	10.62 ± 0.02

In Figure 2, the frozen fraction and number of active sites per cm², n_s , as a function of temperature, is shown. Aside from the sieved and milled wüstite (FeO) samples, all the other iron oxide samples are similar in their ice nucleation activity. From the frozen fraction data in Figure 2a, it can be seen that the iron oxide samples have higher ice nucleation activity than that of background freezing. In Figure 2b, n_s was calculated and showed a stark difference between wüstite (FeO) and the other iron oxide samples. The freezing onset of wüstite (FeO) at -7 °C is unusually warm for an inorganic compound. This temperature is on par with the ice nucleation temperature ranges of biological materials, which have been shown to be some of the best ice nuclei.^{7,21}

K-feldspar, another inorganic compound, has been observed to nucleate ice as warm as -2 °C, which is warmer than found with wüstite (FeO).⁶³ The mechanism that causes ice nucleation in feldspar is likely different than in wüstite (FeO). For feldspar, the perthitic texture has been found as one of the underlying reasons for its ice nucleation activity. Strain from the phase separation of Na⁺ and K⁺ rich domains create crystallographic dislocations that can create surface features for water to be attracted to and then initiate ice nucleation.^{3,14,42} In comparison to bacteria and feldspar, wüstite (FeO) does not possess ice nucleating proteins, and the simplicity of the

crystal structure limits the creation of multiple types of domains to attract water and promote ice nucleation.



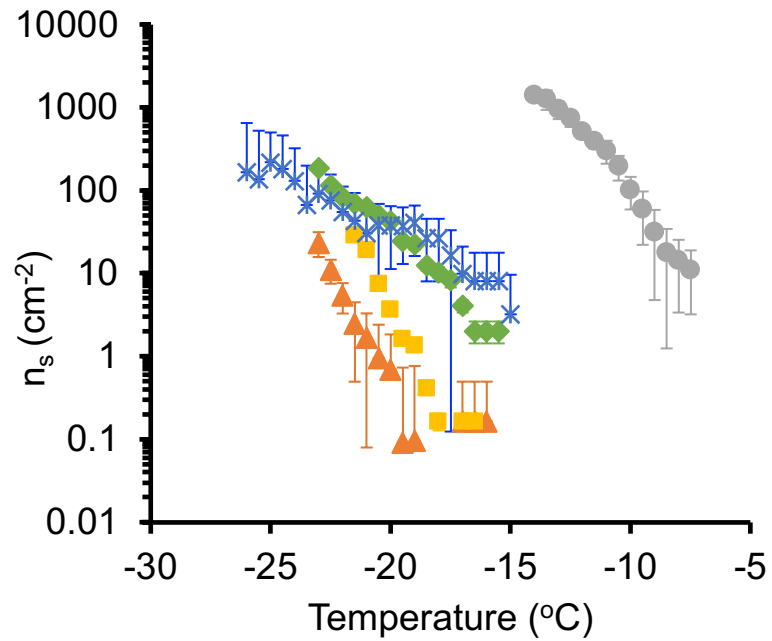


Figure 2. (a) The frozen fraction of the iron oxide samples and the background freezing of UHPLC-MS water, and (b) the number of active sites per cm^2 (n_s) as a function of temperature for the same samples. The figures share a legend

Previous research has found that a high lattice match between the ice structure and the crystal structure of a particle can promote ice nucleation.⁴⁷ In Table 2, the lattice parameters were found using whole pattern fitting using Jade and its libraries. From there, the lattice mismatch along the a, b, and c-axis was calculated from Equation (4) with respect to hexagonal ice, Ih. AgI and corundum were included for comparison. Corundum was found in a previous study to be the best sample among the aluminum oxide samples tested.⁴⁷ Figure S1 shows the lattice mismatch values compared to cubic ice. In Figure 3, the number of active sites at -20 °C, except for wüstite (FeO) which is at -19 °C, are plotted against the lattice mismatch along the a- and b-axis. For most of the samples, the lattice mismatch values are well above 5.7 % except for the a-axis of goethite and the a- and b-axis of wüstite (FeO). Goethite has a similar ice nucleation activity to hematite and magnetite, which indicates that the low lattice mismatch along the a-axis did not affect the ice nucleation activity. On the other hand, wüstite has a lattice mismatch of -4.24 % along the a and b-axis. The negative lattice mismatch indicates that the water molecules in the hexagonal ice lattice would have to compress to template along the surface, which is unfavorable because of the repulsive interactions between water molecules during compression. Nevertheless, the lattice mismatch is low, which may indicate that the repulsion from the compression is sufficiently small that ice nucleation is still improved by the low lattice mismatch. Lattice mismatch with respect to cubic ice was calculated in Table S1.

Table 2. The lattice mismatch along the a-, b-, and c-axis of the iron oxide samples with respect to hexagonal ice, Ih, to three significant figures.

	Lattice parameters ^c			Lattice mismatch along the axis		
	a	b	С	a (%)	b (%)	c (%)
$I_h{}^a$	4.50	4.50	7.32	-	-	-
AgI ^a	4.68	4.68	7.66	4.07	4.07	4.69
Corundum ^b [α-Al ₂ O ₃] (Hexagonal)	4.77	4.77	13.0	6.07	6.07	77.9
Hematite [Fe ₂ O ₃] (Hexagonal)	5.03	5.03	13.8	12.0	12.0	88.0
Magnetite [Fe ₃ O ₄] (Hexagonal)	5.93	5.93	14.6	31.8	31.8	99.0
Goethite [FeOOH] (Orthorhombic)	4.61	9.99	3.03	2.63	122	-58.6
Wüstite [FeO] (Cubic)	4.31	4.31	4.31	-4.24	-4.24	-41.2

 $^{^{}a}$ The lattice parameters of I_{h} and AgI were obtained from Cox et al. (2012). 26 b The lattice parameters of corundum were taken from Chong et al. (2019). 47

^cThe lattice parameters for the samples and corundum were determined from whole pattern fitting using Jade software.

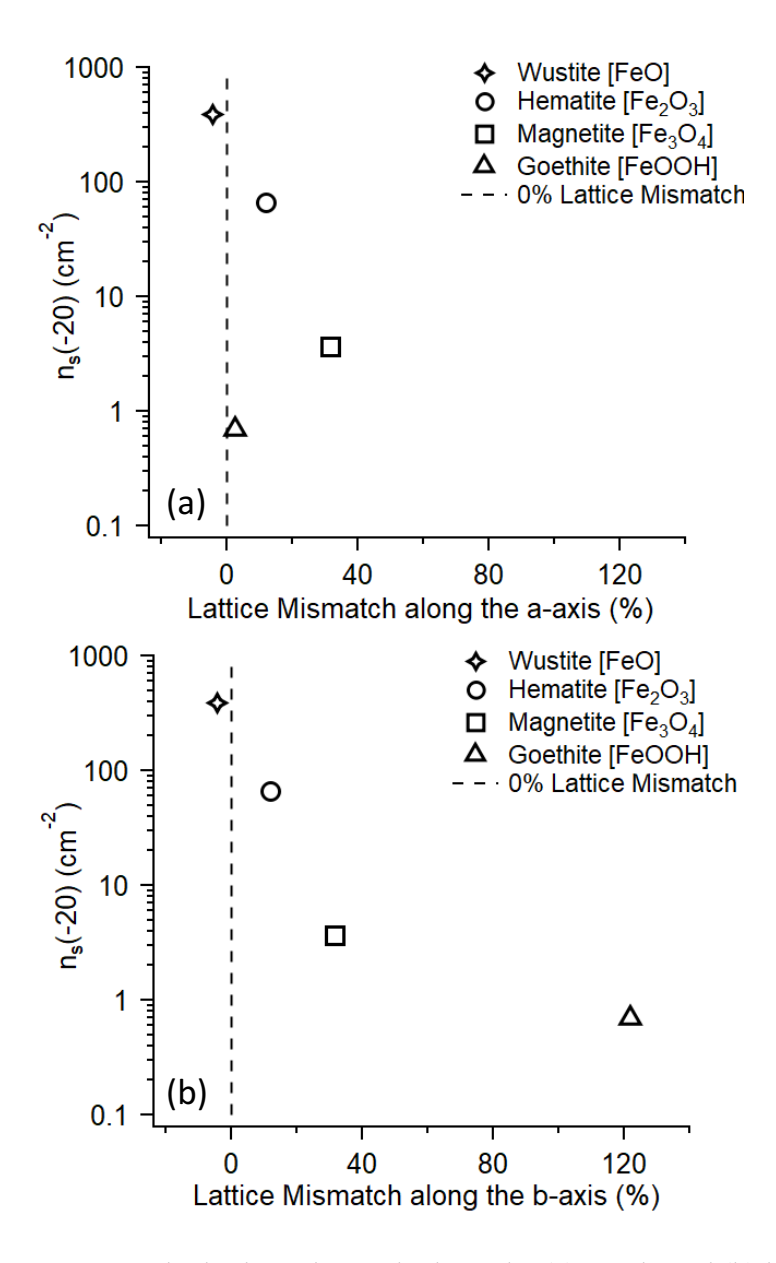


Figure 3. The lattice mismatch along the (a) a-axis and (b) b-axis are shown relative to the number of active sites at -20 °C for each of the iron oxides except for wüstite (FeO) which is at -19 °C. The dotted line correlates to a 0% lattice mismatch.

In addition to lattice match, physical defects at the surface can have a significant impact on the ice nucleation activity. In this study, relatively large pellets of wüstite (FeO) had to be processed further to disperse in water for the ice nucleation experiments. During milling, the wüstite crystallites are ground to micron-sized particles, while preserving the crystal lattice. However, milling can introduce physical defects that, in turn, can affect the ice nucleation activity. In an ESEM study by Kiselev et al., it was seen that ice nucleated along the visible cracks and other defects after repeated experiments, which would suggest that these areas contained active sites for ice nucleation.³ Other studies have shown that certain pore sizes can promote ice nucleation by facilitating hydrogen bonding and inducing a crystal lattice with confined water.^{60,64,65} To examine the effect of milling, MnO powder was prepared in the same fashion as wüstite (FeO). Both minerals have a value of 5.5 on Moh's hardness scale, and as a result, they should have similar mechanical processing from milling.⁶⁶ The ice nucleation data of the milled and sieved samples can be seen in Figure 4. Milled MnO has a slight increase in ice nucleation activity, but it is negligible compared to the increase seen in wüstite (FeO). This result indicates that physical defects alone cannot account for the high ice nucleation activity of milled wüstite (FeO).

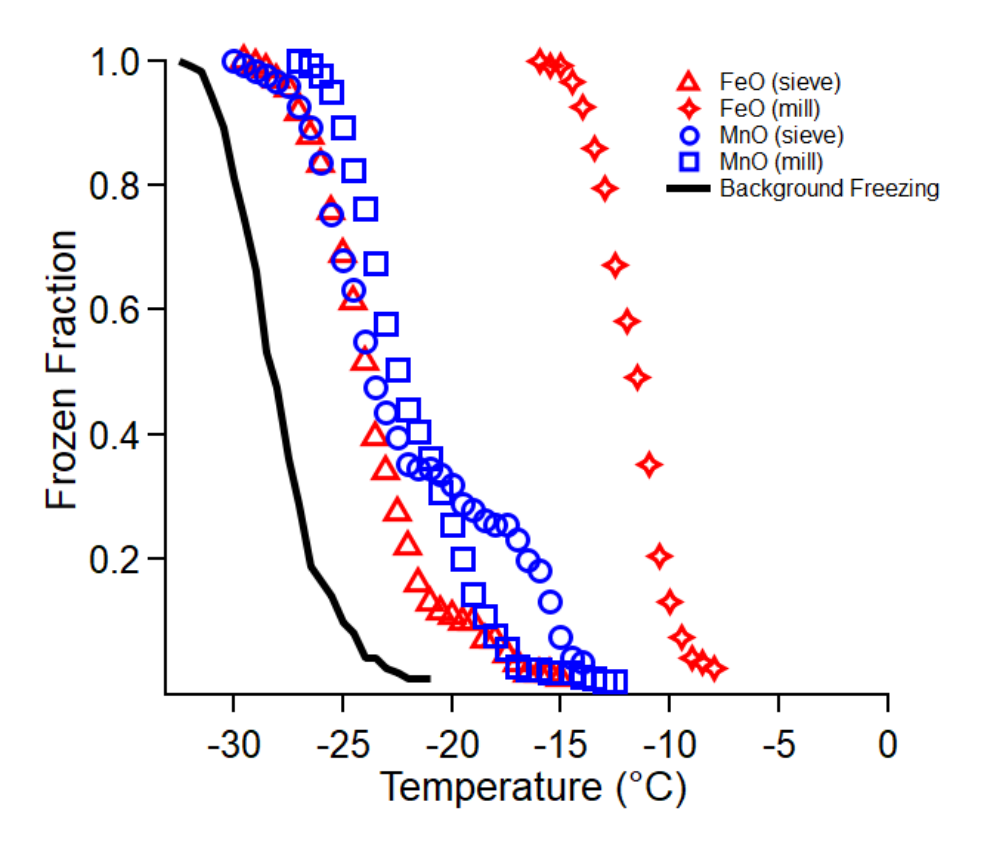


Figure 4. The ice nucleation results of FeO and MnO with two different preparations: milled and 20 μm sieved. The background freezing is UHPLC-MS water.

Because physical defects alone could not explain the ice nucleation activity of wüstite, potential chemical origins were explored. In Table 3, the XPS results are shown for the iron oxides and MnO. From XPS, the concentration of certain surface functional groups such as C-O and Fe-OH of the samples can be compared. Carbon and O-C can be found as contamination on all of the samples. Even with rigorous cleaning and storage under vacuum, adventitious carbon coatings form readily on surfaces. However, in ice nucleation studies with organic coatings, it is found that coatings need to have sufficient coverage over the particles to result in an overall decrease in ice nucleation. Thus, the contamination is not taken into consideration. Besides the organic contaminants, oxygen and metal species were found at the surface. The XPS results of three different wüstite (FeO) samples can be seen. Two milled samples were used: a more freshly milled

wüstite (FeO) sample, tested 1-week after milling, and an older milled sample, tested 2-months after milling. The purpose of these two samples was to determine the stability of any newly exposed functional groups that arise from milling. Interestingly, a higher Fe-OH concentration is found in the 1-week sample compared to the 2-month sample. The Fe-OH concentration was 11.9 % for the 2-month sample, which is comparable to the 10.9% Fe-OH for the 20 µm sieved wüstite (FeO). In comparison, the milled MnO and sieved MnO are similar in their percentages of Mn-OH. The higher Fe-OH density found in the freshly milled wüstite (FeO) compared to the sieved sample suggests that the higher percentage of hydroxyls promotes ice nucleation; whereas the MnO samples have comparable Mn-OH densities and ice nucleation activities. Goethite, however, has the highest Fe-OH percentage, yet it does not show a high ice nucleation activity. While this result may be partially due to lattice match, the relationship between the number of hydroxyl groups and ice nucleation activity is not straightforward. Studies by Lupi et al. and Cox et al. have shown that a high concentration of hydroxyls at the surface can impede ice nucleation.^{69,70} Thus, the high concentration of hydroxyls on goethite may be be detrimental for ice nucleation. Additionally, Pedevilla et al. found through a series of MD simulations that it was not the arrangement of OH groups or the relationship of the OH pattern to ice that influenced ice nucleation, but the OH group density and the substrate-water interaction strength which varies between samples. Furthermore, they found for that for kaolinite, the OH density increased along cracks and edges where covalent bonds are broken and hydroxylated, which may explain why freshly milled FeO has the better ice nucleation activity. 71 On the other hand, magnetite has similar Fe-OH concentration as 1-week milled wüstite (FeO) but has worse ice nucleation activity. Simulations have shown that hydroxyls may be a contributing factor to ice nucleation activity by increasing the wettability of a surface. From these simulations, the ability of water molecules to

orient into an ice-like lattice was found to be more important.^{11,69} Therefore, freshly milled wüstite (FeO) seems to have enough hydroxyls to hydrogen bond with water molecules as well as a good lattice match with hexagonal ice along the a- and b-axis that will allow for templating of the water molecules into an ice-like lattice.

Table 3. The XPS results of the iron oxide samples and MnO.

	Concentration (atom %)					
Sample	C	Fe/Mn	О-С	O-(Fe, Mn)	OH-(Fe, Mn)	
FeO milled (1 week)	18.7	25.1	7.6	32.0	16.6	
FeO milled (2 months)	19.5	22.9	10.2	35.5	11.9	
FeO (20 μm sieve)	16.9	27.3	2.8	42.1	10.9	
Hematite [Fe ₂ O ₃]	12.8	30.3	5.4	42.2	9.2	
Magnetite [Fe ₃ O ₄]	11.1	26.7	2.2	42.4	17.6	
Goethite [FeOOH]	11.2	24.9	3.0	26.0	34.9	
MnO milled	18.1	24.7	4.9	40.5	11.8	
MnO (20 μm sieve)	18.1	25.6	3.6	40.2	12.4	

CONCLUSION

In this study, the ice nucleation activities of several atmospherically relevant iron oxides were compared. Within the iron oxide system studied, hematite (Fe₂O₃), goethite (FeOOH), and magnetite (Fe₃O₄) had similar ice nucleation activities, which may be attributed to the high lattice mismatch with hexagonal ice. Wüstite (FeO) was observed to have surprisingly high ice nucleation

activity, which is higher than many atmospheric mineral dust particles.^{7,15} Although not atmospherically relevant like the other iron oxide samples, wüstite (FeO) was chosen because of its high lattice match with hexagonal ice. The lattice mismatch of wüstite (FeO) along the a- and b-axes was shown to be low, although the ice lattice would have to compress to fit the template along the wüstite (FeO) crystal lattice. Repulsion forces result in compression of the ice lattice, which is unfavorable. Nonetheless, the compression may be sufficiently small that the high degree of lattice match promotes ice nucleation. Because wüstite (FeO) was the only sample that required milling, comparison studies with sieved wüstite (FeO) and milled and sieved MnO were used to observe the effect of physical defects on ice nucleation activity. The sieved and milled MnO had comparable ice nucleation activities with the milled sample showing a slight increase. From the comparison with MnO, it was concluded that the physical defects were not the only contributing factor for the high ice nucleation activity of the milled wüstite (FeO). XPS analysis showed that freshly milled wüstite (FeO) had a higher concentration of hydroxyls compared to the sieved wüstite (FeO), which may promote the ice nucleation process. In addition, the Fe-OH concentration of the freshly milled, 1-week old wüstite (FeO), is greater than the 2-month old milled wüstite (FeO), which suggests that the newly exposed hydroxyls are not stable over a long time period. The milling of wüstite (FeO) provided insight into improving ice nucleation activity of particles using mechanical force to expose functional groups. Overall, the ice nucleation activity of wüstite (FeO) may be a result of a combination of the increased site density of hydroxyl groups caused by milling and the high lattice match along the a- and b-axes.

The findings from this study have provided further insights into the mechanisms of heterogeneous ice nucleation. Specifically, the processing that the particles undergo before ice nucleation experiments can have a significant impact on their ice nucleation activities. In

laboratory experiments, the samples are often processed by milling, grinding with a mortar and pestle, or other mechanical forces. Although the physical defects may or may not contribute to the ice nucleation, processing could change the functional groups at the newly exposed surfaces, which could possibly change the ice nucleation activity. In a broader sense, atmospheric particles often experience aging and processing the atmosphere. As such, changes to the surface properties of atmospheric particles after processing and their effect on the site density of functional groups at the surface could be an important factor when considering the ice nucleation activity in cloud models. The exposure of functional groups after mechanical processes can have potential important impacts on ice nucleation and warrants further investigation.

AUTHOR INFORMATION

Supporting Information

A table of the lattice parameters of the cubic ice and iron oxide samples and the lattice mismatch with respect to cubic ice for each of the iron oxide samples.

Corresponding Author

* To whom all correspondence should be addressed: maf43@psu.edu, 814-867-4267

Author Contributions

The manuscript was written through contributions of all authors. All authors have given approval to the final version of the manuscript.

Conflicts of Interest

The authors declare no competing financial interests.

ACKNOWLEDGEMENTS

We gratefully acknowledge support from an NSF CAREER award (CHE 1351383) and NSF CHE-1904803. We also acknowledge the Materials Characterization Lab at the Pennsylvania State University for instrument use (XRD, XPS, and BET), E. Bazilevskaya for the BET data, and J. Shallenberger for the XPS data.

REFERENCES

- (1) Pruppacher, H. R.; Klett, J. D. Heterogeneous Nucleation; 2010; pp 287–360. https://doi.org/10.1007/978-0-306-48100-0_9.
- (2) Atkinson, J. D.; Murray, B. J.; Woodhouse, M. T.; Whale, T. F.; Baustian, K. J.; Carslaw, K. S.; Dobbie, S.; O'Sullivan, D.; Malkin, T. L. The Importance of Feldspar for Ice Nucleation by Mineral Dust in Mixed-Phase Clouds. *Nature* **2013**, *498* (7454), 355–358. https://doi.org/10.1038/nature12278.
- (3) Kiselev, A.; Bachmann, F.; Pedevilla, P.; Cox, S. J.; Michaelides, A.; Gerthsen, D.; Leisner, T. Active Sites in Heterogeneous Ice Nucleation-the Example of K-Rich Feldspars. *Science* **2016**, *355* (6323), 367–371. https://doi.org/10.1126/science.aai8034.
- (4) DeMott, P. J.; Prenni, A. J.; McMeeking, G. R.; Sullivan, R. C.; Petters, M. D.; Tobo, Y.; Niemand, M.; Möhler, O.; Snider, J. R.; Wang, Z.; Kreidenweis, S. M. Integrating Laboratory and Field Data to Quantify the Immersion Freezing Ice Nucleation Activity of Mineral Dust Particles. *Atmospheric Chemistry and Physics* **2015**, *15* (1), 393–409. https://doi.org/10.5194/acp-15-393-2015.
- (5) Augustin-Bauditz, S.; Wex, H.; Kanter, S.; Ebert, M.; Niedermeier, D.; Stolz, F.; Prager, A.; Stratmann, F. The Immersion Mode Ice Nucleation Behavior of Mineral Dusts: A Comparison of Different Pure and Surface Modified Dusts. *Geophysical Research Letters* **2014**, *41* (20), 7375–7382. https://doi.org/10.1002/2014GL061317.
- (6) Archuleta, C. M.; DeMott, P. J.; Kreidenweis, S. M. Ice Nucleation by Surrogates for Atmospheric Mineral Dust and Mineral Dust/Sulfate Particles at Cirrus Temperatures. *Atmospheric Chemistry and Physics* **2005**, *5* (10), 2617–2634. https://doi.org/10.5194/acp-5-2617-2005.
- (7) Morris, C. E.; Georgakopoulos, D. G.; Sands, D. C. Ice Nucleation Active Bacteria and Their Potential Role in Precipitation. *Journal de Physique IV (Proceedings)* **2004**, *121*, 87–103. https://doi.org/10.1051/jp4:2004121004.
- (8) Szyrmer, W.; Zawadzki, I.; Szyrmer, W.; Zawadzki, I. Biogenic and Anthropogenic Sources of Ice-Forming Nuclei: A Review. https://doi.org/10.1175/1520-0477(1997)078<0209:BAASOI>2.0.CO;2 1997. https://doi.org/10.1175/1520-0477(1997)078<0209:BAASOI>2.0.CO;2.
- (9) Wilson, T. W.; Ladino, L. A.; Alpert, P. A.; Breckels, M. N.; Brooks, I. M.; Browse, J.; Burrows, S. M.; Carslaw, K. S.; Huffman, J. A.; Judd, C.; Kilthau, W. P.; Mason, R. H.; McFiggans, G.; Miller, L. A.; Najera, J. J.; Polishchuk, E.; Rae, S.; Schiller, C. L.; Si, M.; Temprado, J. V.; Whale, T. F.; Wong, J. P. S.; Wurl, O.; Yakobi-Hancock, J. D.; Abbatt, J. P. D.; Aller, J. Y.; Bertram, A. K.; Knopf, D. A.; Murray, B. J. A Marine Biogenic Source of Atmospheric Ice-Nucleating Particles. *Nature* 2015, 525 (7568), 234–238. https://doi.org/10.1038/nature14986.
- (10) Diehl, K.; Quick, C.; Matthias-Maser, S.; Mitra, S. K.; Jaenicke, R. The Ice Nucleating Ability of Pollen Part I: Laboratory Studies in Deposition and Condensation Freezing Modes. *Atmospheric Research* **2001**, *58* (2), 75–87. https://doi.org/10.1016/S0169-8095(01)00091-6.
- (11) Lupi, L.; Hudait, A.; Molinero, V. Heterogeneous Nucleation of Ice on Carbon Surfaces. *Journal of the American Chemical Society* **2014**, *136* (8), 3156–3164. https://doi.org/10.1021/ja411507a.
- (12) Möhler, O.; Linke, C.; Saathoff, H.; Schnaiter, M.; Wagner, R.; Mangold, A.; Krämer, M.; Schurath, U. Ice Nucleation on Flame Soot Aerosol of Different Organic Carbon Content. *Meteorologische Zeitschrift* 2005, 14 (4), 477–484. https://doi.org/10.1127/0941-2948/2005/0055.
- (13) Friedman, B.; Kulkarni, G.; Beránek, J.; Zelenyuk, A.; Thornton, J. A.; Cziczo, D. J. Ice Nucleation and Droplet Formation by Bare and Coated Soot Particles. *Journal of Geophysical Research* **2011**, *116* (D17), D17203. https://doi.org/10.1029/2011JD015999.
- (14) Hoose, C.; Möhler, O. Heterogeneous Ice Nucleation on Atmospheric Aerosols: A Review of Results from Laboratory Experiments. *Atmos. Chem. Phys* **2012**, *12*, 9817–9854. https://doi.org/10.5194/acp-12-9817-2012.

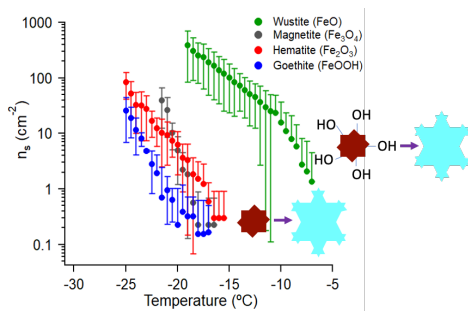
- (15) Murray, B. J.; O'Sullivan, D.; Atkinson, J. D.; Webb, M. E. Ice Nucleation by Particles Immersed in Supercooled Cloud Droplets. *Chemical Society Reviews*. Royal Society of Chemistry October 7, 2012, pp 6519–6554. https://doi.org/10.1039/c2cs35200a.
- (16) Eickhoff, L.; Dreischmeier, K.; Zipori, A.; Sirotinskaya, V.; Adar, C.; Reicher, N.; Braslavsky, I.; Rudich, Y.; Koop, T. Contrasting Behavior of Antifreeze Proteins: Ice Growth Inhibitors and Ice Nucleation Promoters. *Journal of Physical Chemistry Letters* 2019, 10 (5), 966–972. https://doi.org/10.1021/acs.jpclett.8b03719.
- (17) O'Sullivan, D.; Murray, B. J.; Ross, J. F.; Whale, T. F.; Price, H. C.; Atkinson, J. D.; Umo, N. S.; Webb, M. E. The Relevance of Nanoscale Biological Fragments for Ice Nucleation in Clouds. *Scientific Reports* 2015, 5 (1), 1–7. https://doi.org/10.1038/srep08082.
- (18) Joly, M.; Attard, E.; Sancelme, M.; Deguillaume, L.; Guilbaud, C.; Morris, C. E.; Amato, P.; Delort, A. M. Ice Nucleation Activity of Bacteria Isolated from Cloud Water. *Atmospheric Environment* 2013, 70, 392–400. https://doi.org/10.1016/j.atmosenv.2013.01.027.
- (19) Pratt, K. A.; DeMott, P. J.; French, J. R.; Wang, Z.; Westphal, D. L.; Heymsfield, A. J.; Twohy, C. H.; Prenni, A. J.; Prather, K. A. In Situ Detection of Biological Particles in Cloud Ice-Crystals. *Nature Geoscience* **2009**, *2* (6), 398–401. https://doi.org/10.1038/ngeo521.
- (20) Rangel-Alvarado, R. B.; Nazarenko, Y.; Ariya, P. A. Snow-Borne Nanosized Particles: Abundance, Distribution, Composition, and Significance in Ice Nucleation Processes. *Journal of Geophysical Research: Atmospheres* 2015, 120 (22), 11,760-11,774. https://doi.org/10.1002/2015JD023773.
- (21) Möhler, O.; Demott, P. J.; Vali, G.; Levin, Z. *Microbiology and Atmospheric Processes: The Role of Biological Particles in Cloud Physics*; 2007; Vol. 4.
- (22) Choobari, O. A.; Zawar-Reza, P.; Sturman, A. The Global Distribution of Mineral Dust and Its Impacts on the Climate System: A Review. *Atmospheric Research*. Elsevier Ltd March 1, 2014, pp 152–165. https://doi.org/10.1016/j.atmosres.2013.11.007.
- (23) Cahill, C. F. Asian Aerosol Transport to Alaska during ACE-Asia. *Journal of Geophysical Research D: Atmospheres* **2003**, *108* (23). https://doi.org/10.1029/2002jd003271.
- (24) Pruppacher, H. R.; Klett, J. D. *Microphysics of Clouds and Precipitation*; Kluwer Academic Publishers, 1997.
- (25) Fitzner, M.; Sosso, G. C.; Cox, S. J.; Michaelides, A. The Many Faces of Heterogeneous Ice Nucleation: Interplay Between Surface Morphology and Hydrophobicity. *Journal of the American Chemical Society* **2015**, *137* (42), 13658–13669. https://doi.org/10.1021/jacs.5b08748.
- (26) Cox, S. J.; Kathmann, S. M.; Purton, J. A.; Gillan, M. J.; Michaelides, A. Non-Hexagonal Ice at Hexagonal Surfaces: The Role of Lattice Mismatch. *Physical Chemistry Chemical Physics* **2012**, *14* (22), 7944. https://doi.org/10.1039/c2cp23438f.
- (27) Hsiao, P.-Y.; Tsai, Z.-H.; Huang, J.-H.; Yu, G.-P. Strong Asymmetric Effect of Lattice Mismatch on Epilayer Structure in Thin-Film Deposition. *Physical Review B* **2009**, *79* (15), 155414. https://doi.org/10.1103/PhysRevB.79.155414.
- (28) Glatz, B.; Sarupria, S. Heterogeneous Ice Nucleation: Interplay of Surface Properties and Their Impact on Water Orientations. *Langmuir* **2018**, *34* (3), 1190–1198. https://doi.org/10.1021/acs.langmuir.7b02859.
- (29) Hu, X. L.; Michaelides, A. Ice Formation on Kaolinite: Lattice Match or Amphoterism? *Surface Science* **2007**, *601* (23), 5378–5381. https://doi.org/10.1016/J.SUSC.2007.09.012.
- (30) Thürmer, K.; Nie, S. Formation of Hexagonal and Cubic Ice during Low-Temperature Growth. *Proceedings of the National Academy of Sciences of the United States of America* **2013**, *110* (29), 11757–11762. https://doi.org/10.1073/pnas.1303001110.
- (31) Marcolli, C.; Nagare, B.; Welti, A.; Lohmann, U. Ice Nucleation Efficiency of AgI: Review and New Insights. *Atmospheric Chemistry and Physics* **2016**, *16* (14), 8915–8937. https://doi.org/10.5194/acp-16-8915-2016.

- (32) DeMott, P. J. Quantitative Descriptions of Ice Formation Mechanisms of Silver Iodide-Type Aerosols. *Atmospheric Research* **1995**, *38* (1–4), 63–99. https://doi.org/10.1016/0169-8095(94)00088-U.
- (33) Zielke, S. A.; Bertram, A. K.; Patey, G. N. A Molecular Mechanism of Ice Nucleation on Model Agl Surfaces. *The Journal of Physical Chemistry B* **2015**, *119* (29), 9049–9055. https://doi.org/10.1021/jp508601s.
- (34) Feibelman, P. J. Lattice Match in Density Functional Calculations: Ice Ih vs. β-Agl. *Physical Chemistry Chemical Physics* **2008**, *10* (32), 4688. https://doi.org/10.1039/b808482n.
- (35) Qiu, Y.; Odendahl, N.; Hudait, A.; Mason, R.; Bertram, A. K.; Paesani, F.; DeMott, P. J.; Molinero, V. Ice Nucleation Efficiency of Hydroxylated Organic Surfaces Is Controlled by Their Structural Fluctuations and Mismatch to Ice. *Journal of the American Chemical Society* **2017**, *139* (8), 3052–3064. https://doi.org/10.1021/jacs.6b12210.
- (36) Conrad, P.; Ewing, G. E.; Karlinsey, R. L.; Sadtchenko, V. Ice Nucleation on BaF 2(111). *Journal of Chemical Physics* **2005**, *122* (6), 064709. https://doi.org/10.1063/1.1844393.
- (37) Bi, Y.; Cao, B.; Li, T. Enhanced Heterogeneous Ice Nucleation by Special Surface Geometry. *Nature Communications* **2017**, *8*, 15372. https://doi.org/10.1038/ncomms15372.
- (38) Pinti, V.; Marcolli, C.; Zobrist, B.; Hoyle, C. R.; Peter, T.; Pinti, V.; Marcolli, C.; Zobrist, B.; Hoyle, C. R.; Peter, T. Ice Nucleation Efficiency of Clay Minerals in the Immersion Mode ETH Library Ice Nucleation Efficiency of Clay Minerals in the Immersion Mode. *Atmospheric Chemistry and Physics* **2012**, *12* (13), 5859–5878. https://doi.org/10.3929/ethz-b-000052156.
- (39) Campbell, J. M.; Meldrum, F. C.; Christenson, H. K. Observing the Formation of Ice and Organic Crystals in Active Sites. *Proceedings of the National Academy of Sciences of the United States of America* **2017**, *114* (5), 810–815. https://doi.org/10.1073/pnas.1617717114.
- (40) Campbell, J. M.; Christenson, H. K. Nucleation- and Emergence-Limited Growth of Ice from Pores. *Physical Review Letters* **2018**, *120* (16), 165701. https://doi.org/10.1103/PhysRevLett.120.165701.
- (41) Pach, E.; Verdaguer, A. Pores Dominate Ice Nucleation on Feldspars. *Journal of Physical Chemistry C* **2019**, *123* (34), 20998–21004. https://doi.org/10.1021/acs.jpcc.9b05845.
- (42) Peckhaus, A.; Kiselev, A.; Hiron, T.; Ebert, M.; Leisner, T. A Comparative Study of K-Rich and Na/Ca-Rich Feldspar Ice-Nucleating Particles in a Nanoliter Droplet Freezing Assay. *Atmospheric Chemistry and Physics* **2016**, *16* (18), 11477–11496. https://doi.org/10.5194/acp-16-11477-2016.
- (43) Holden, M. A.; Whale, T. F.; Tarn, M. D.; O'Sullivan, D.; Walshaw, R. D.; Murray, B. J.; Meldrum, F. C.; Christenson, H. K. High-Speed Imaging of Ice Nucleation in Water Proves the Existence of Active Sites. *Science Advances* **2019**, *5* (2), eaav4316. https://doi.org/10.1126/sciadv.aav4316.
- (44) Whale, T. F.; Holden, M. A.; Kulak, A. N.; Kim, Y.-Y.; Meldrum, F. C.; Christenson, H. K.; Murray, B. J. The Role of Phase Separation and Related Topography in the Exceptional Ice-Nucleating Ability of Alkali Feldspars. *Physical Chemistry Chemical Physics* 2017, 19 (46), 31186–31193. https://doi.org/10.1039/C7CP04898J.
- (45) Hiranuma, N.; Hoffmann, N.; Kiselev, A.; Dreyer, A.; Zhang, K.; Kulkarni, G.; Koop, T.; Möhler, O. Influence of Surface Morphology on the Immersion Mode Ice Nucleation Efficiency of Hematite Particles. Atmospheric Chemistry and Physics 2014, 14 (5), 2315–2324. https://doi.org/10.5194/acp-14-2315-2014.
- (46) Zolles, T.; Burkart, J.; Häusler, T.; Pummer, B.; Hitzenberger, R.; Grothe, H. Identification of Ice Nucleation Active Sites on Feldspar Dust Particles. *Journal of Physical Chemistry A* **2015**, *119* (11), 2692–2700. https://doi.org/10.1021/jp509839x.
- (47) Chong, E.; King, M.; Marak, K. E.; Freedman, M. A. The Effect of Crystallinity and Crystal Structure on the Immersion Freezing of Alumina. *Journal of Physical Chemistry A* **2019**, *123* (12), 2447–2456. https://doi.org/10.1021/acs.jpca.8b12258.

- (48) Prasad, P. S. R.; Shiva Prasad, K.; Krishna Chaitanya, V.; Babu, E. V. S. S. K.; Sreedhar, B.; Ramana Murthy, S. In Situ FTIR Study on the Dehydration of Natural Goethite. *Journal of Asian Earth Sciences* **2006**, *27* (4), 503–511. https://doi.org/10.1016/j.jseaes.2005.05.005.
- (49) Nadoll, P.; Angerer, T.; Mauk, J. L.; French, D.; Walshe, J. The Chemistry of Hydrothermal Magnetite: A Review. *Ore Geology Reviews*. Elsevier September 1, 2014, pp 1–32. https://doi.org/10.1016/j.oregeorev.2013.12.013.
- (50) Fischer, R. A.; Campbell, A. J.; Shofner, G. A.; Lord, O. T.; Dera, P.; Prakapenka, V. B. Equation of State and Phase Diagram of FeO. *Earth and Planetary Science Letters* **2011**, *304* (3–4), 496–502. https://doi.org/10.1016/j.epsl.2011.02.025.
- (51) Gleeson, B.; Hadavi, S. M. M.; Young, D. J. Isothermal Transformation Behavior of Thermally-Grown Wustite. *Materials at High Temperatures* **2000**, *17* (2), 311–318. https://doi.org/10.1179/mht.2000.17.2.020.
- (52) Guieu, C. Chemical Characterization of the Saharan Dust End-Member: Some Biogeochemical Implications for the Western Mediterranean Sea. *Journal of Geophysical Research* 2002, 107 (D15), 4258. https://doi.org/10.1029/2001JD000582.
- (53) Martin, J. H.; Fitzwater, S. E.; Gordon, R. M. Iron Deficiency Limits Phytoplankton Growth in Antarctic Waters. *Global Biogeochemical Cycles* **1990**, *4* (1), 5–12. https://doi.org/10.1029/GB004i001p00005.
- (54) Mahowald, N. M.; Baker, A. R.; Bergametti, G.; Brooks, N.; Duce, R. A.; Jickells, T. D.; Kubilay, N.; Prospero, J. M.; Tegen, I. Atmospheric Global Dust Cycle and Iron Inputs to the Ocean. *Global Biogeochemical Cycles*. John Wiley & Sons, Ltd December 1, 2005. https://doi.org/10.1029/2004GB002402.
- (55) Schulz, M.; Prospero, J. M.; Baker, A. R.; Dentener, F.; Ickes, L.; Liss, P. S.; Mahowald, N. M.; Nickovic, S.; García-Pando, C. P.; Rodríguez, S.; Sarin, M.; Tegen, I.; Duce, R. A. Atmospheric Transport and Deposition of Mineral Dust to the Ocean: Implications for Research Needs. *Environmental Science and Technology*. American Chemical Society October 2, 2012, pp 10390– 10404. https://doi.org/10.1021/es300073u.
- (56) Tagliabue, A.; Bowie, A. R.; Boyd, P. W.; Buck, K. N.; Johnson, K. S.; Saito, M. A. The Integral Role of Iron in Ocean Biogeochemistry. *Nature*. Nature Publishing Group March 1, 2017, pp 51–59. https://doi.org/10.1038/nature21058.
- (57) Ito, A.; Myriokefalitakis, S.; Kanakidou, M.; Mahowald, N. M.; Scanza, R. A.; Hamilton, D. S.; Baker, A. R.; Jickells, T.; Sarin, M.; Bikkina, S.; Gao, Y.; Shelley, R. U.; Buck, C. S.; Landing, W. M.; Bowie, A. R.; Perron, M. M. G.; Guieu, C.; Meskhidze, N.; Johnson, M. S.; Feng, Y.; Kok, J. F.; Nenes, A.; Duce, R. A. Pyrogenic Iron: The Missing Link to High Iron Solubility in Aerosols. *Science Advances* 2019, 5 (5), eaau7671. https://doi.org/10.1126/sciadv.aau7671.
- (58) Cwiertny, D. M.; Baltrusaitis, J.; Hunter, G. J.; Laskin, A.; Scherer, M. M.; Grassian, V. H. Characterization and Acid-Mobilization Study of Iron-Containing Mineral Dust Source Materials. *Journal of Geophysical Research: Atmospheres* **2008**, *113* (D5), n/a-n/a. https://doi.org/10.1029/2007JD009332.
- (59) Brunauer, S.; Emmett, P. H.; Teller, E. Adsorption of Gases in Multimolecular Layers. *Journal of the American Chemical Society* **1938**, *60* (2), 309–319. https://doi.org/10.1021/ja01269a023.
- (60) Alstadt, V. J.; Dawson, J. N.; Losey, D. J.; Sihvonen, S. K.; Freedman, M. A. Heterogeneous Freezing of Carbon Nanotubes: A Model System for Pore Condensation and Freezing in the Atmosphere. The Journal of Physical Chemistry A 2017, 121 (42), 8166–8175. https://doi.org/10.1021/acs.jpca.7b06359.
- (61) Vali, G.; Vali, G. Quantitative Evaluation of Experimental Results and the Heterogeneous Freezing Nucleation of Supercooled Liquids. *Journal of the Atmospheric Sciences* **1971**, *28* (3), 402–409. https://doi.org/10.1175/1520-0469(1971)028<0402:QEOERA>2.0.CO;2.

- (62) Bi, Y.; Cabriolu, R.; Li, T. Heterogeneous Ice Nucleation Controlled by the Coupling of Surface Crystallinity and Surface Hydrophilicity. *The Journal of Physical Chemistry C* **2016**, *120* (3), 1507–1514. https://doi.org/10.1021/acs.jpcc.5b09740.
- (63) Harrison, A. D.; Whale, T. F.; Carpenter, M. A.; Holden, M. A.; Neve, L.; O'Sullivan, D.; Vergara Temprado, J.; Murray, B. J. Not All Feldspars Are Equal: A Survey of Ice Nucleating Properties across the Feldspar Group of Minerals. *Atmospheric Chemistry and Physics*. Copernicus GmbH September 5, 2016, pp 10927–10940. https://doi.org/10.5194/acp-16-10927-2016.
- (64) Tombari, E.; Johari, G. P. On the State of Water in 2.4 Nm Cylindrical Pores of MCM from Dynamic and Normal Specific Heat Studies. *Journal of Chemical Physics* **2013**, *139* (6), 064507. https://doi.org/10.1063/1.4817333.
- (65) Dore, J. Structural Studies of Water in Confined Geometry by Neutron Diffraction. *Chemical Physics* **2000**, *258* (2–3), 327–347. https://doi.org/10.1016/S0301-0104(00)00208-1.
- (66) Anthony, J. W.; Bideaux, R. A.; Bladh, K. W.; Nichols, M. C. *Handbook of Mineralogy*; Mineralogical Society of America: Chantilly, VA 20151-1110, USA.
- (67) Möhler, O.; Benz, S.; Saathoff, H.; Schnaiter, M.; Wagner, R.; Schneider, J.; Walter, S.; Ebert, V.; Wagner, S. The Effect of Organic Coating on the Heterogeneous Ice Nucleation Efficiency of Mineral Dust Aerosols. *Environmental Research Letters* 2008, 3 (2), 25007. https://doi.org/10.1088/1748-9326/3/2/025007.
- (68) Yang, Z.; Bertram, A. K.; Chou, K. C. Why Do Sulfuric Acid Coatings Influence the Ice Nucleation Properties of Mineral Dust Particles in the Atmosphere? *Journal of Physical Chemistry Letters* **2011**, *2* (11), 1232–1236. https://doi.org/10.1021/jz2003342.
- (69) Lupi, L.; Molinero, V. Does Hydrophilicity of Carbon Particles Improve Their Ice Nucleation Ability? Journal of Physical Chemistry A **2014**, 118 (35), 7330–7337. https://doi.org/10.1021/jp4118375.
- (70) Cox, S. J.; Kathmann, S. M.; Slater, B.; Michaelides, A. Molecular Simulations of Heterogeneous Ice Nucleation. I. Controlling Ice Nucleation through Surface Hydrophilicity. *The Journal of Chemical Physics* **2015**, *142* (18), 184704. https://doi.org/10.1063/1.4919714.
- (71) Pedevilla, P.; Fitzner, M.; Michaelides, A. What Makes a Good Descriptor for Heterogeneous Ice Nucleation on OH-Patterned Surfaces. *Phys. Rev. B* **2017**, *96* (11), 115441. https://doi.org/10.1103/PhysRevB.96.115441.

Table of Contents Entry



FeO has enhanced ice nucleation activity due to functional groups that are exposed upon mechanical processing.